

CODEN STJSAO  
ZX470/1549ISSN 0562-1887  
UDK 620.196.2:621.785.3

# Intergranular corrosion of dissimilar austenitic weld

**Branko MATEŠA<sup>1)</sup>, Ivan SAMARDŽIĆ<sup>2)</sup>  
and Marko DUNĐER<sup>2)</sup>**

1) Strojarški fakultet u Slavonskom Brodu,  
Sveučilište J.J. Strossmayera u Osijeku  
(Mechanical Engineering Faculty in  
Slavonski Brod, J.J. Strossmayer University  
of Osijek), Trg Ivane Brlić Mažuranić 2,  
HR-35000 Slavonski Brod,  
**Republic of Croatia**

2) Filozofski fakultet Sveučilišta u Rijeci,  
Odsjek za politehniku (Faculty of  
Philosophy, University of Rijeka,  
Department of Polytechnic), Omladinska  
14, HR- 51000 Rijeka,  
**Republic of Croatia**

bmatesa@gmail.com

## Keywords

*Intergranular corrosion*  
*Dissimilar austenitic weld*  
*Delta-ferrite*  
*Heat treatment by annealing*  
*Huey test*

## Ključne riječi

*Međukristalna korozija*  
*Austenitni raznovrsni zavar*  
*Delta-ferit*  
*Toplinska obradba žarenjem*  
*Huey test*

**Primljeno (Received):** 2011-03-24

**Prihvaćeno (Accepted):** 2011-06-28

## 1. Introduction

At dissimilar stainless steels weld local sensitized zones (i.e., regions susceptible to corrosion) often are developed. Due to the formation of chromium carbide along grain boundaries, sensitization results in depletion of chromium in the region adjacent to the grain boundary. The region will be sensitized to corrosion, resulting in inter-granular attack. Inter-granular corrosion causes a loss of metal in a region that parallels the weld deposit. This corrosion behaviour is called weld decay and schematic review of chromium depleted zones caused by carbide precipitation on grain boundaries is shown on Figure 1. The minimum time required for carbide formation sensitization as a function of carbon content in a typical stainless steel alloy is shown on Figure 2. The figure shows

Original scientific paper

Research on influence of heat treatment parameters by annealing (temperature and time duration) as well as quality of austenitic stainless steel weld joint of dissimilar steel on degree delta ferrite transformation (measured by device for ferrite content measuring dr.Foerster type 1.053) and inter-granular corrosion rate using Huey test (ASTM A 262 part C). A pair of basic materials quality in accordance with standards ASTM A387Gr.12 and ASTM A 240 TP 304L was welded by SMAW using austenitic consumable material different quality. Factors plan of experiment 3<sup>3</sup> has been applied i.e. temperature 650, 700, 750 °C; time duration 0, 2, 10 hours and welds quality AWS E309L, AWS E316L, AWS E 308L.

## Međukristalna korozija raznovrsnog austenitnog zavara

Izvorno znanstveni članak

Provedena su istraživanja utjecaja parametara toplinske obradbe žarenjem (temperature i vremena trajanja) te vrste austenitnog korozijski postojanog zavarenog spoja raznovrsnih čelika na stupanj transformacije delta ferita (mjereno uređajem za određivanje sadržaja ferita dr.Foerster tip 1.053) i brzinu međukristalne korozije putem Huey testa (ASTM A 262 part C). Par osnovnih materijala kakvoće sukladne normama ASTM A387gr.12 i ASTM A240 TP 304L zavarivan je REL postupkom primjenom austenitnog dodatnog materijala različite kakvoće. Primijenjen je faktorski plan pokusa 3<sup>3</sup>, tj. varirane su razine temperature toplinske obradbe žarenjem 650, 700, 750 °C, kao i vrijeme trajanja toplinske obradbe 0, 2, 10 sati te kakvoća zavarenog spoja raznovrsnih čelika AWS E309L, AWS E316L, AWS E 308L.

susceptibility to sensitization as a function of temperature, time and carbon content.

At very low cooling rates, the formation of chromium carbide occurs at higher temperature resulting in a more extensive chromium- depleted region. Because of the fact that the normal welding thermal cycle is finished in approximately two minutes, the carbon content have to not exceed 0,08 wt % to avoid sensitization.

The control of stainless steel weld sensitization may be achieved by using:

- A post-weld high-temperature annealing and
- quenching to dissolve the chromium at grain boundaries, and prevent chromium carbide formation on cooling
- A low-carbon grade of stainless steel (e.g. AISI 304L or AISI 316L) to avoid carbide formation

Symbols/Oznake			
AISI	- American Iron and Steel Institute - Američki Institut željezo i čelik	A	- Austenitic single phase solidification mode ( $\gamma$ ) - Austenitni oblik skrutnjavanja faza( $\gamma$ )
ASTM	- American Society for Testing and Materials - Američka Udruga za ispitivanje i materijale	AF	- Primary phase ( $\gamma$ ) + Eutectic Ferrite( $\delta$ ) - Primarna austenitna faza ( $\gamma$ ) + eutektički ferit ( $\delta$ )
AWS	- American Welding Society - Američka zavarivačka udruga	FA	- Primary phase ( $\delta$ ) + Peryectic/ Eutectic Phase ( $\gamma$ ) - Primarna feritna faza( $\delta$ ) + Peritektička/Eutektička austenitna faza ( $\gamma$ )
I	- Welding current strength, A - Jakost struje zavarivanja	F	- $\delta$ -Ferrite single phase solidification - $\delta$ - feritna faza skrutnjavanja
U	- Voltage of welding current, V - Napon struje zavarivanja	v	- Welding velocity, cm/min - Brzina zavarivanja
$\sigma$ - phase	- Brittle Fe-Cr intermetallic phase with more than 50 % Cr. - Krhki intermetalni Fe-Cr spoj s više od 50 % Cr.	q	- Specific heat input by welding - Specifični unos topline zavarivanja, kJ/cm
$\chi$ -phase	- Chi-phase (Fe <sub>36</sub> Cr <sub>12</sub> Mo <sub>10</sub> ) - Či-faza, intermetalni spoj u zavaru s molibdenom.	"	- Coefficient efficiency, % - Stupanj djelotvornosti

- A stabilized grade of stainless steel containing titanium (alloy AISI 321) or niobium (alloy AISI 347), which preferentially form carbides and leave chromium in solution. (There is the possibility of knife-line attack in stabilized grades of stainless steel.)
- A high-chromium alloy (e.g., alloy AISI 310).

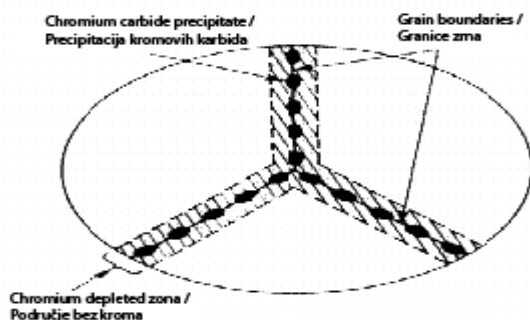


**Figure 1.** Schematic review of chromium depleted, sensitised zones caused by carbide precipitation on grain boundaries [1]

**Slika 1.** Shematski prikaz područja bez kroma uzrokovanih stvaranjem karbida na granicama zrna [1]

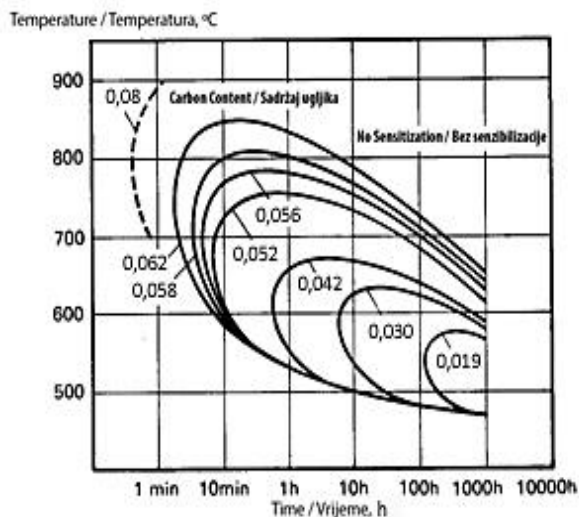


**Figure 2.** Time-temperature-sensitization diagram as a function of carbon content for a typical 300-series stainless steel alloy [2]

**Slika 2.** Dijagram vrijeme-temperatura-sklonost kao ovisnosti o sadržaju ugljika za posebne korozijski postojeće čelike grupe 300 [2]

## 2. Delta Ferrite in Stainless Steel Weld Metals

Austenitic weld metals are frequently used to join dissimilar alloys. It has been established that it is necessary to have austenitic weld deposits solidify as primary ferrite ( $\delta$ -ferrite), if hot cracking is to be minimized. The amount and form of ferrite in the weld metal can be controlled by selecting a filler metal with the appropriate chromium and nickel equivalent. A high chromium-to-nickel ratio favours primary ferrite formation, whereas a low ratio promotes primary austenite (Figure 3).

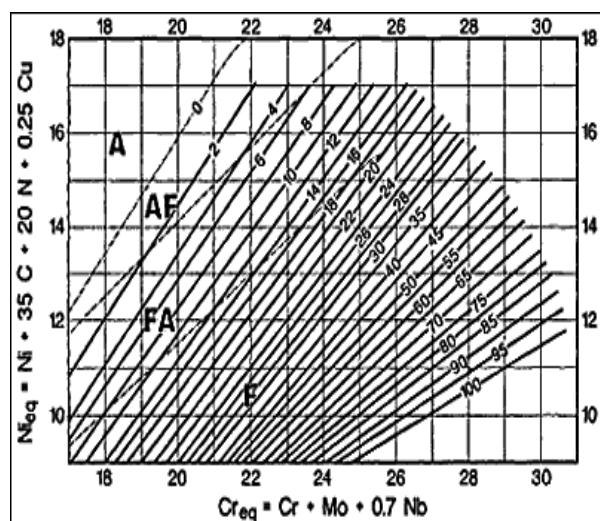


Figure 3. The WRC-1992 diagram [3]

Slika 3. WRC-1992 dijagram [3]

The WRC-1992 diagram for stainless steel weld metals has been recognized by the International Institute of Welding (IIW) as the most accurate and preferred constitution diagram for estimating or predicting ferrite in nominally austenitic and duplex ferrite-austenite stainless steel weld metals [4].

This diagram shows the compositional range for the desirable primary solidification mode. The dotted lines on the diagram indicate the various transitions in the primary solidification phase. Because not all ferrite is primary ferrite (i.e., some is a phase component of a ferrite-austenite eutectic), this diagram can be used to ensure that ferrite is the first solid (primary) phase to form. This condition occurs when the weld deposit has a composition in the range labelled FA in Figure 3. Because primary ferrite is the preferable microstructure, use of this diagram should reduce problems of hot cracking during welding. Also, the corrosion behaviour of stainless steel welds is measurably different depending on whether the stainless steel has a microstructure generated with primary ferrite or primary austenite. The knowledge of the weld metal ferrite

content and form is necessary in order to be able to properly characterize and predict corrosion behaviour of dissimilar austenitic metal welds [5].

## 3. Experiments

Research on influence of heat treatment parameters by annealing (temperature and time duration) as well as quality of austenitic stainless steel weld joint of dissimilar steel on delta ferrite transformation and intergranular corrosion rate is performed.

Delta-ferrite contents in dissimilar austenitic welds are determined by dr. Foerster-Institute Ferrite Content - Meter type 1.054 device which work on eddy current basis. Measuring was performed on six different places of specimens purposed for examination of inter-granular corrosion favourable dimensions 22 x 6 x 4 mm.

Huey-test is corrosion test for evaluating intergranular corrosion resistance by boiling in refluxed 65 % nitric acid (ASTM A262, Practice C). The specimens are boiled for five consecutive periods, each of 48 hours. The corrosion rate (mm/year) during each boiling period is calculated from the decrease in the weight of the specimens. The Huey test environment is strongly oxidizing, and, is used as a check on whether the material has been correctly heat treated. This test is suitable for the detection of chromium depleted regions as well as intermetallic precipitations, like  $\sigma$ -phase as well as  $\chi$ -phase, in the material. The Huey test is also used for materials that come into contact with strongly oxidising agents, e.g. nitric acid. This procedure may also be used to check the effectiveness of stabilizing elements and of reductions in carbon content in reducing susceptibility to inter granular attack in chromium-nickel stainless welds. The test was performed on minimum three (3) specimens for each level of experiment.

### 3.1. Plan, parameters and results of experiments

In the experiment the pair of steel which was examined is ASTM A 240TP 304L with ASTM A 387 Gr.12, thickness 10 mm. The pair was welded with three different austenitic SMAW consumable. Table 1 shows chemical analysis of welded base materials for welding. Chemical elements analysis of SMAW consumable material is presented on Table 2. Review of welding parameters is shown on Table 3. Minimum interpass temperature was hold on the level of preheating temperature. Plan of experiment is recognised from Tables 4 and 5. The review of measured and calculated delta-ferrite values is presented on Table 4 with characteristic diagrams on Figure 4. The review of measured and calculated intergranular rate (mm/year) is presented on Table 5 with characteristic flow of diagrams shown on Figures 5-6.

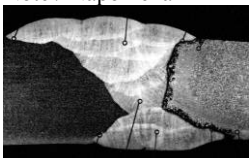
**Table 1.** Chemical elements analysis of base materials for welding**Tablica 1.** Kemijska analiza elemenata osnovnih materijala za zavarivanje

The base material for welding / Osnovni materijal za zavarivanje	Chemical elements contents / Kemijski sadržaj elemenata, wt %								
	C	Si	Mn	P	S	Cr	Mo	Ni	Fe
ASTM A 387 Gr.12	0,12	0,26	0,54	0,009	0,011	0,99	0,48	-	Rem.
ASTM A 240 TP 304L	0,020	0,53	1,45	0,033	0,033	18,9	-	10,1	Rem.

**Table 2.** Chemical elements analysis of SMAW consumable material**Tablica 2.** Kemijska analiza elemenata dodatnih materijala za REL zavarivanje

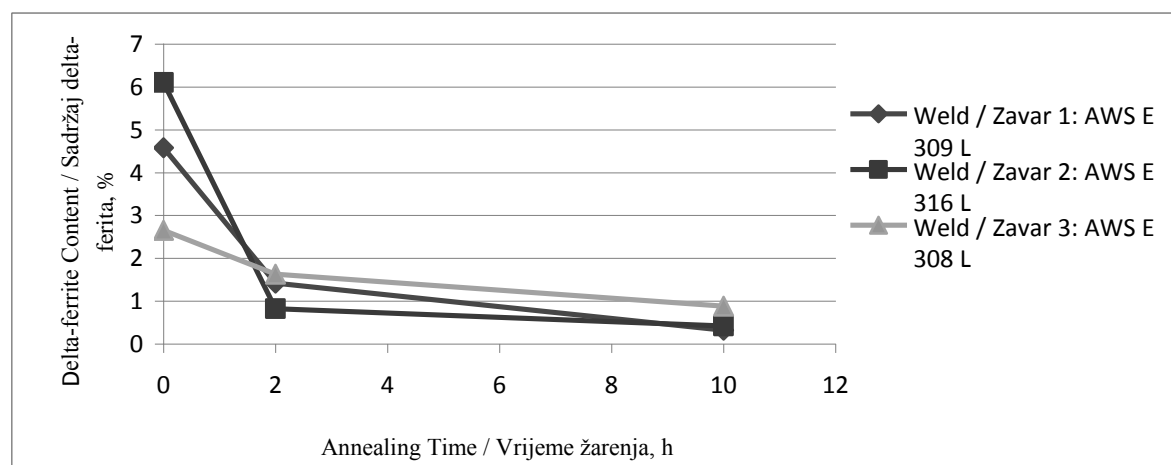
SMAW consumable material / dodatni materijal za REL zavarivanje	Elements contents / Sadržaj elemenata, wt %								
	C	Si	Mn	Ni	Cr	Mo	S	P	Fe
AWS E 309 L	0,019	0,85	0,83	13,3	23,3	-	0,011	0,022	Rem.
AWS E 316 L	0,019	1,03	0,55	11,0	18,8	2,82	0,003	0,023	Rem.
AWS E 308 L	0,030	0,80	0,60	9,20	19,1	-	0,060	0,060	Rem.

**Table 3.** Review of welding parameters**Tablica 3.** Pregled parametara zavarivanja

SMAW Consumable / Dodatni materijal za REL zavarivanje	AWS E 309 L	AWS E 316 L	AWS E 308 L
Tension of welding current Napon struje zavarivanja $U, V$	25 - 26	25 - 26	25 - 26
Strength of welding current / Jakost struje zavarivanja $I, A$	90 - 100	90 - 110	95 - 110
Welding velocity / Brzina zavarivanja $v, cm/min$	15 - 32	19 - 35	15 - 32
Preheating temperature / Temperatura predgijavanja $T_{pr.}, ^\circ C$	150 - 160	150 - 160	150 - 160
Specific heat input by welding /Specifični unos topline zavarivanja $q = \frac{UI}{1000v} 60 \eta,$ kJ/cm...(1) $\eta = 0,7$ (SMAW/ REL zavar.)	3,37-7,28	2,71 - 5,35	3,37 - 7
Number of layers	11	12	13
Average specific heat input /Prosječni specifični unos topline pri	4,8	4,0	4,8
Note / Napomena 	All basic coated electrodes before welding are baked on 250-300 °C minimum 2 hours. After 8 <sup>th</sup> layer welding the root was grind and welded from other side. / Sve bazične elektrode prije zavarivanja su sušene na 250-300 °C najmanje 2 sata. Nakon zavarivanja 8-og sloja, korijen je brušen i zavaren s druge strane.		

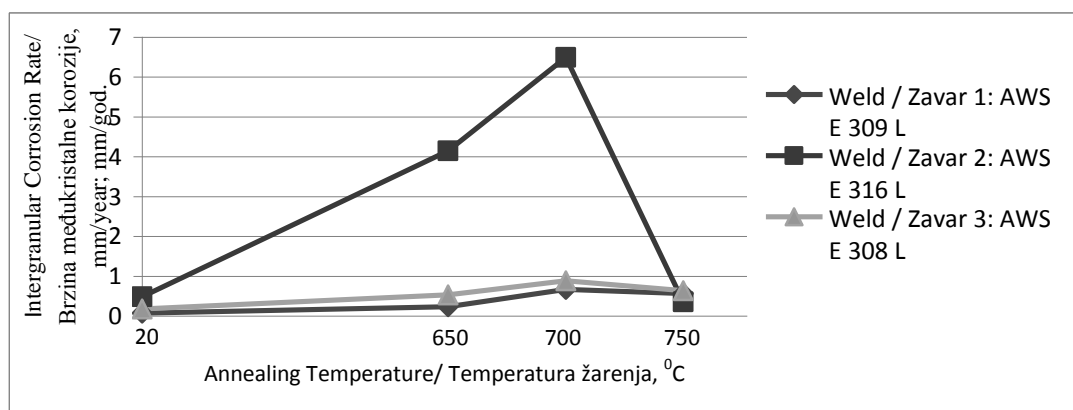
**Table 4.** Review of average values  $\bar{X}$  of  $\delta$ -ferrite measured in welds, %**Tablica 4.** Pregled srednjih vrijednosti  $\bar{X}$   $\delta$ -ferita mjerenih u zavaru, %

Consumable SMAW material / Dodatni materijal za REL zavarivanje A	Annealing time / Vrijeme žarenja C, h	C <sub>1</sub> = 0 h No annealing Bez žarenja		C <sub>2</sub> = 2 h		C <sub>3</sub> = 10 h	
		Annealing temperature/ Temperatura žarenja B, °C					
A <sub>1</sub> AWS E 309 L	B <sub>1</sub> 650 °C	5,00	$\bar{X} = 4,58$	2,25	$\bar{X} = 2,37$	0,15	$\bar{X} = 1,84$
		4,85		2,30		2,25	
		3,90		2,50		3,10	
B <sub>2</sub> 700 °C	5,00	$\bar{X} = 4,58$	1,35	$\bar{X} = 1,44$	1,55	$\bar{X} = 0,22$	
	4,85		1,70		1,05		
	3,90		1,25		1,05		
B <sub>3</sub> 750 °C	5,00	$\bar{X} = 4,58$	0,80	$\bar{X} = 1,42$	0,45	$\bar{X} = 0,32$	
	4,85		1,75		0,30		
	3,90		1,70		0,20		
A <sub>2</sub> AWS E 316 L	B <sub>1</sub> 650 °C	6,35	$\bar{X} = 6,10$	3,35	$\bar{X} = 3,10$	0,45	$\bar{X} = 2,53$
		6,20		3,20		3,80	
		5,75		2,85		3,35	
B <sub>2</sub> 700 °C	6,35	$\bar{X} = 6,10$	2,18	$\bar{X} = 2,04$	2,80	$\bar{X} = 2,43$	
	6,20		2,60		3,10		
	5,75		1,35		1,40		
B <sub>3</sub> 750 °C	6,35	$\bar{X} = 6,10$	0,75	$\bar{X} = 0,82$	0,40	$\bar{X} = 0,42$	
	6,20		0,75		0,40		
	5,75		0,95		0,45		
A <sub>3</sub> AWS E 308 L	B <sub>1</sub> 650 °C	2,35	$\bar{X} = 2,65$	2,30	$\bar{X} = 2,72$	3,00	$\bar{X} = 3,1$
		3,45		2,50		3,60	
		2,15		3,35		2,70	
B <sub>2</sub> 700 °C	2,35	$\bar{X} = 2,65$	1,25	$\bar{X} = 1,85$	2,15	$\bar{X} = 1,57$	
	3,45		2,05		1,40		
	2,15		2,25		1,15		
B <sub>3</sub> 750 °C	2,35	$\bar{X} = 2,65$	2,10	$\bar{X} = 1,63$	0,95	$\bar{X} = 0,88$	
	3,45		0,85		0,85		
	2,15		1,95		0,85		

**Figure 4.** Diagram delta-ferrite transformation after annealing on 750 °C**Slika 4.** Dijagram transformacije delta-ferita nakon žarenja na 750 °C

**Table 5.** Review of average values  $\bar{X}$  of intergranular corrosion test of welds (ASTM A 262 part C)**Tablica 5.** Pregled srednjih vrijednosti  $\bar{X}$  testa međukristalne korozije u zavaru (ASTM A 262 dio C)

Consumable SMAW material / Dodatni materijal za REL zavarivanje A	Annealing time / Vrijeme žarenja C, h  Annealing temperature/ Temperatura žarenja B, °C	C <sub>1</sub> = 0 h  No annealing Bez žarenja		C <sub>2</sub> = 2 h		C <sub>3</sub> = 10 h	
			$\bar{X}$		$\bar{X}$		$\bar{X}$
A <sub>1</sub> AWS E 309 L	B <sub>1</sub> 650 °C	0,09 0,08 0,05	$\bar{X}$ = 0,073	0,19 0,24 0,27	$\bar{X}$ = 0,233	1,77 3,54 3,81	$\bar{X}$ = 3,04
	B <sub>2</sub> 700 °C	0,09 0,08 0,05	$\bar{X}$ = 0,073	1,00 0,55 0,45	$\bar{X}$ = 0,667	1,48 1,28 0,69	$\bar{X}$ = 1,15
	B <sub>3</sub> 750 °C	0,09 0,08 0,05	$\bar{X}$ = 0,073	1,04 0,37 0,27	$\bar{X}$ = 0,560	0,25 0,54 0,27	$\bar{X}$ = 0,353
A <sub>2</sub> AWS E 316 L	B <sub>1</sub> 650 °C	0,49 0,51 0,45	$\bar{X}$ = 0,483	5,12 3,87 3,44	$\bar{X}$ = 4,143	1,65 6,52 4,88	$\bar{X}$ = 4,35
	B <sub>2</sub> 700 °C	0,49 0,51 0,45	$\bar{X}$ = 0,483	8,80 6,31 4,36	$\bar{X}$ = 6,490	0,51 1,28 3,24	$\bar{X}$ = 1,667
	B <sub>3</sub> 750 °C	0,49 0,51 0,45	$\bar{X}$ = 0,483	0,30 0,38 0,39	$\bar{X}$ = 0,357	0,58 0,55 0,63	$\bar{X}$ = 0,587
A <sub>3</sub> AWS E 308 L	B <sub>1</sub> 650 °C	0,24 0,15 0,15	$\bar{X}$ = 0,180	0,54 0,54 0,52	$\bar{X}$ = 0,533	0,50 1,55 0,32	$\bar{X}$ = 0,790
	B <sub>2</sub> 700 °C	0,24 0,15 0,15	$\bar{X}$ = 0,180	0,54 0,52 1,60	$\bar{X}$ = 0,887	0,85 1,00 2,05	$\bar{X}$ = 1,30
	B <sub>3</sub> 750 °C	0,24 0,15 0,15	$\bar{X}$ = 0,180	0,36 1,10 0,45	$\bar{X}$ = 0,637	0,74 0,81 0,39	$\bar{X}$ = 0,647

**Figure 5.** Diagram of intergranular corrosion rate of dissimilar austenitic welds at annealing duration of 2 hours**Slika 5.** Dijagram brzine međukristalne korozije austenitnog raznorodnog zavaru pri žarenju kroz 2 sata

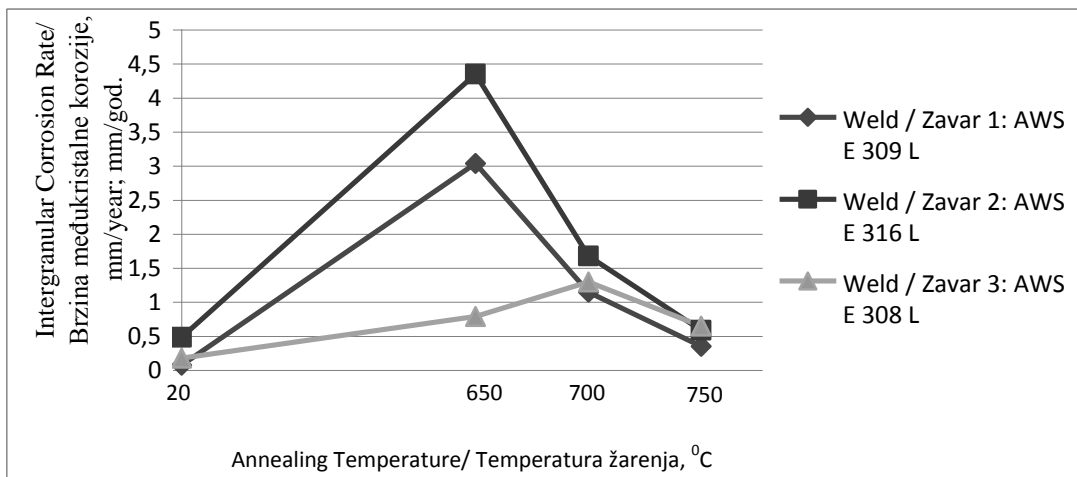


**Figure 6.** Diagram of intergranular corrosion rate of dissimilar austenitic welds ( mm/year) at annealing duration of 10 h

**Slika 6.** Dijagram brzine medukristalne korozije raznorodnog austenitnog zavara (mm/god) pri trajanju žarenja od 10 sati

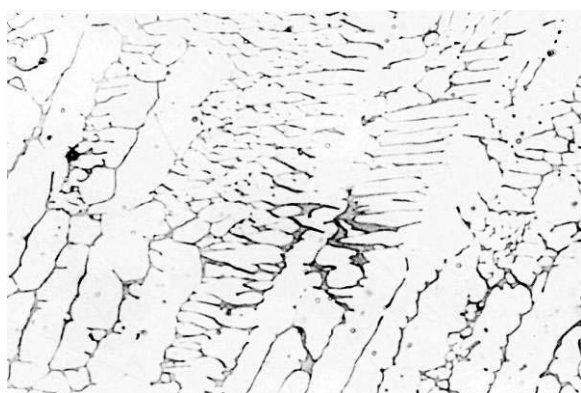


**Figure 7.** Microstructure of SMAW AWS E 316L weld, as welded state, 5 % KOH electrolytic , 500x

**Slika 7.** Mikrostruktura REL zavara s dodatnim materijalom AWS E 316L, u zavarenom stanje, elektrolitički nagrizano u 5 % KOH, 500x

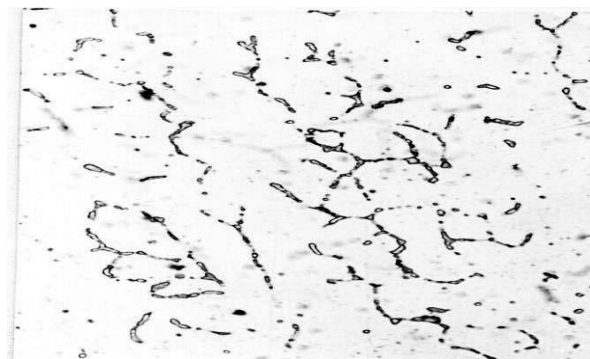


**Figure 8.** Microstructure of SMAW AWS E 316L weld, annealed at 750 C/10 hours, 5%KOH electrolytic , 500x

**Slika 8.** Mikrostruktura REL zavara s dodatnim materijalom AWS E 316L, žareno na 750 °C/10 sati, elektrolitički nagrizano u 5 % KOH, 500x

The characteristic microstructures of dissimilar austenitic welds with  $\delta$ -ferrite transformations to carbide  $Cr_{23}C_6$ ,  $\sigma$ - and  $\chi$ -phase are shown on Figures 7-8. On Figures 9-10 welds decay caused by intergranular corrosion is shown.

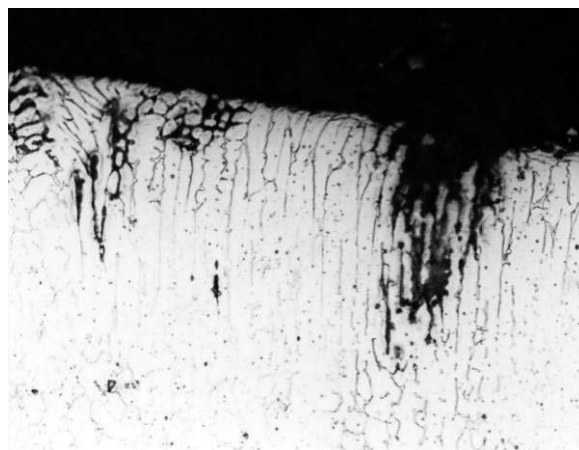


**Figure 9.** Microstructure SMAW weld AWSE 316L, as welded state, after Huey corrosion test, Glicergya, 200x

**Slika 9.** Mikrostruktura REL zavara s dodatnim materijalom AWS E316L u zavarenom stanju, nakon provedenog Huey testa, Glicergya, 200x

In as welded state of AWS E316L weld corrosion damage along dendritic grains and alpha-phase is in places to 150  $\mu$ m in depth. Further corrosion damage at annealing on 650 °C/10 hours of weld retains the basic intergranular nature but the intensity of decay is considerable larger.

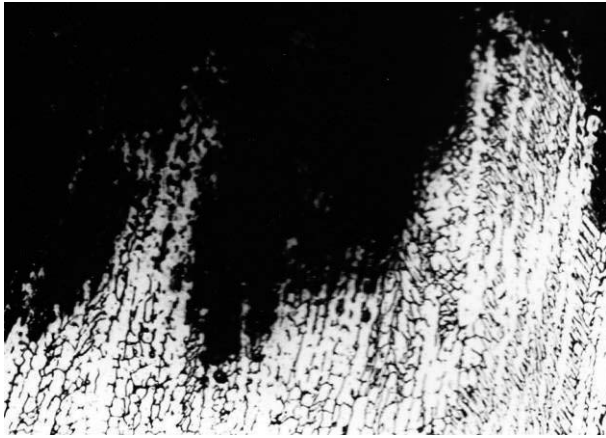


**Figure 10.** Microstructure SMAW weld AWS E 316L annealing on 650 °C/10 hours, Glicergya, 200x

**Slika 10.** Mikrostruktura REL zavara s dodatnim materijalom AWS E 316L, žarenog na 650 °C/10 sati, Glicergya, 200x

#### 4. Discussion

Depending on the chemical composition, delta ferrite is transformed completely or only partially into sigma phase with small amount of residual ferrite remaining in most cases. With longer annealing times, sigma phase is also precipitated from austenite. Finally, the structure consists of four phases, i.e. austenite, carbide  $M_{23}C_6$ , sigma phase and residual delta ferrite. Sigma phase is not ferro-magnetic and its precipitation by way of delta ferrite decay can be measured with the aid of a magnetic ferrite measuring device. In molybdenum containing chrome-nickel austenite weld steel, the chromium-iron mixed carbide  $M_{23}C_6$  is precipitated first at 750 °C. With prolonged annealing times, this carbides picks up molybdenum which, being a carbide forming element, becomes increasingly dissolved in  $M_{23}C_6$ , with a simultaneous drop in carbon content. First, iron-carbon-molybdenum mixed carbides are formed which are then converted to the chi phase ( $Fe_{36}Cr_{12}Mo_{10}$ ) with about 1% Cr. With increasing molybdenum content,  $M_{23}C_6$  precipitation and intergranular corrosion attack becomes increasingly influenced by precipitation and intermetallic phases.

#### 5. Conclusions

Investigations of heat treatment by annealing influence as well as quality of dissimilar austenitic metal weld on transformation degree of delta ferrite in weld, it could be concluded as follows:

The time of heat treatment duration has more significant influence on transformation rate in relation on heat treatment temperature.

The most part of delta-ferrite transformation take place already after 2 hours annealing regardless off temperature.

The specimens with larger amount of delta-ferrite in as welded state (welded by consumable material quality of AWS E 316L) show the highest transformation degree what was specially expressed at prolonged duration time of 10 hours.

Analysing the influence of heat treatment by annealing on intergranular corrosion favour of austenitic dissimilar weld joints can be concluded the following: Significant influence of the annealing parameters: temperature and time duration on intergranular corrosion rate.

Specifically, the time duration influence more than temperature on corrosion rate.

Regarding to use austenitic dissimilar weld quality, the highest corrosion rate is present at joints welded with AWS E 316L, as well as the lowest at AWS E 309L joints.

#### REFERENCES

- [1] GOOCH, T. G., WILLINGHAM, D.C., *Weld Decay in AISI 304 Stainless Steel*, Metal Construction.& British Welding Journal, Vol 3, No. 10, (1971), 366-372.
- [2] DAVIDSON, R.M., DE BOLD, T. , JOHNSON M.J., *Metals Handbook*, Vol 13, 9th ed., ASM International, 1987, p 551
- [3] KOTECKI, D.J., SIEWERT, T. A.: *WRC-1992 constitution diagram for stainless steel weld metals: a modification of the WRC-1988 diagram*, Welding Journal, 71, (1992), 5, 171-178.
- [4] LEFEBVRE, J.: *Guidance on specifications of ferrite in stainless steel weld metal*, Welding in the World, 31, (1993), 6, 390-407.
- [5] HONEYCOMBE, J. , GOOCH, T.G. *Intergranular Attack in Welded Stress-Corrosion Resistant Stainless Steel*, Welding Journal, Vol 56, No. 11, (1977), p 339-353.
- [6] MATEŠA, B. *Istraživanje utjecaja parametara žarenja na strukturna svojstva ručno elektrolučno zavarenog spoja raznorodnih čelika, I. dio*, Zavarivanje, Vol. 34, broj.3/4, svibanj,kolovoz 1991., str. 67-75.
- [7] MATEŠA, B. *Istraživanje utjecaja parametara žarenja na strukturna svojstva ručno elektrolučno zavarenog spoja raznorodnih čelika, II. dio*, Zavarivanje, Vol 35, broj 1, veljača 1992., str. 5-13.